AIAA JOURNAL
Vol. 34, No. 10, October 1996

Local Buckling of Cracked and Pin-Loaded Plates

W. Z. L. Zhuang,* J. P. Baird,† and H. M. Williamson‡
University of New South Wales, Canberra, ACT 2600, Australia

The interaction between buckling and fracture may affect crack growth in thin riveted aircraft fuselage structures. Buckling may also complicate and induce the phenomenon of multisite damage in aircraft fuselages. This buckling-fracture phenomenon in thin-walled structures is studied through an idealized model, a cracked and pin-loaded hole in a plate. Despite this simplification, a better understanding of the mechanisms of fatigue and fracture in thin-walled structures is obtained by a finite element model and an experiment, using holospeckle interferometry. The experimental studies show an interesting phenomenon, the presence of a combination of tearing mode III as well as opening mode I fracture mechanisms at the cracks in the pin-loaded plates after local buckling. This phenomenon is discussed, and further research is foreshadowed.

Introduction

THE fuselage skin of modern jet transports carries as its major loading the cyclical fuselage pressurization loading. This kind of loading can cause fatigue damage to the aircraft hull. The in-flight structural failure of the top half of fuselage section 43 of an Aloha Airlines Boeing 737-200 has been attributed to a longitudinal fracture of the fuselage skin caused by a fatigued lap rivet joint. Postaccident examination of this fuselage revealed that fatigue cracks emanated from successive rivet holes along a longitudinal row. Structural damage that is characterized by small cracks emanating from consecutive holes along rows of loaded rivets is called multisite damage or widespread fatigue damage.[1]

Current metal aircraft design practice allows the skin panels of some structural components (fuselage and stabilizer panels) to buckle under various loading conditions indicated by Frostig et al.[2] In experiments on thin-walled structures subject to tensile loads, discontinuities such as a joint hole, fatigue crack, etc., can cause local buckling as a result of regions of relatively high compressive stresses near the discontinuities. Such buckling near rivets was observed some time ago in the outer skins of Titan rockets by Rader and McGregor.[3] They associated this buckling with the fatigue failure of the skin panels of the rockets.

Therefore, the reliable use of these thin-walled structures in aircraft fuselages will, in a significant way, depend on a thorough understanding of buckling behavior in the development of the fracture. Conversely, the effect that fracture behavior has on the buckled region may also be important.

Tension buckling phenomena have attracted the attention of a number of investigators. For example, a relatively thin flat plate, subject to a concentrated force acting on opposite boundaries, can become buckled as a result of induced compressive regions associated with the points of concentrated loading. However, a flat plate subject to uniform tensile load will not buckle unless a discontinuity or cutout, such as a hole or crack, exists. After theoretically investigating the buckling under tension of a membrane containing a hole, Cherepanov[4] deduced that thin elastic plates containing holes and under tension generally contain regions of compressive stress near the holes. The compressive stresses may attain such a magnitude that, in the regions where they are acting, the plate becomes unstable and buckles.

In numerical investigations, by the aid of finite element methods (FEMs), the buckling of cracked members under tension has been analyzed by Markstrom and Storakers.[5] They considered the effect of biaxial loading for one specific geometry, investigated the buckling behavior of three types of edge cracked members, and stated the interaction of local buckling and fracture. Using the FEM with triangular finite elements, Sih and Lee[6] analyzed the tensile and compressive buckling of plates weakened by cracks (simulated by narrow ellipses). Results for the various buckling displacement modes have been obtained for tensile and compressive loads with the cracks oriented normal and parallel to the loading axis. The critical buckling loads were found to decrease with increasing crack size. Moreover, local wrinkling of the plate surface became less pronounced for the higher buckling modes. A recent study by Shaw and Huang[7] investigated the buckling characteristics of cracked plates subject to uniaxial tensile loads by the aid of the FEM. They showed that crack buckling behavior is affected by the in-plane stress distribution around a crack.

With the foregoing in mind, there are quite a few studies on tension buckling, but all of them do not cover the local buckling problem of a central crack with a pin-loaded hole in the plate. The current investigators realized that the local buckling phenomenon complicates fracture behavior in thin riveted aircraft structures. Since riveted joints in aircraft are complicated by a number of factors such as rivet bypassing and bearing forces, rivet tilt, and the friction associated with rivet clamping forces, it is too difficult to get the theoretical solution. In this paper, a simplified model of a cracked riveted joint, that is a cracked and pin-loaded hole in a plate as shown in Fig. 1, has been used as a starting point for future investigations. This model is studied numerically and experimentally. The finite element studies

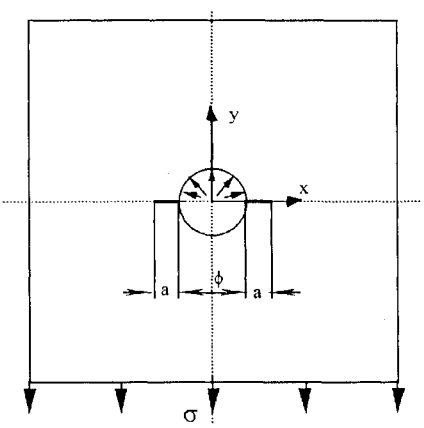

Fig. 1 Cracked and pin-loaded plate.

Received Dec. 23, 1994; revision received Dec. 23, 1995; accepted for publication Feb. 6, 1996.

*Research Associate, Department of Aerospace and Mechanical Engineering, University College, Australian Defence Force Academy; currently Research Scientist, Airframes and Engines Division, Defence Science and Technology Organization, 506 Lorimer Street, Fishermens' Bend, Melbourne 3207, Australia.

†Associate Professor, Department of Aerospace and Mechanical Engineering, University College, Australian Defence Force Academy.

‡Senior Lecturer, Department of Aerospace and Mechanical Engineering, University College, Australian Defence Force Academy.

provide estimates of the prebuckling stress field and then predict buckling loads and mode shapes from the stress field. Finally, experimental studies of plates with cracked, pin-loaded holes are conducted using holographic interferometry to measure displacements. The buckling loads and mode shapes measured in the experimental studies are compared with the preceding finite element studies.

The experimental studies confirm the presence of local buckling in a cracked and pin-loaded structure. The experiments also show that, in these circumstances, the fracture behavior of the cracks is heavily influenced by the buckling and consists of a combination of the expected opening mode (mode I) plus the tearing mode (mode III).

Numerical Analysis

Prebuckling Stress Analysis

Since the prebuckling in-plane stress field in the plate determines the local buckling, the in-plane stress of the pin-loaded plate should be calculated first. The finite element codes used herein for calculation were written by Zhuang et al.[8]

The finite element model used in this investigation of local buckling of a cracked and pin-loaded plate is illustrated in Fig. 2. Pin loading is modeled by a cosine pressure distribution on the upper half of the hole since the cosine pressure distribution is closer to the case of the pin contacting than a uniform pressure distribution. Cases with and without the crack have been modeled using a finite element program that uses the Mindlin plate theory in the formulation of the elements.

There are two main reasons that we chose Mindlin plate theory to analyze the local buckling of pin-loaded plate. First, C_1 continuity is no longer required so that it is easy to implement in conventional displacement-type finite element programming. Second, Mindlin plate theory allows for transverse shear deformation effects and thus offers an attractive alternative to classical Kirchhoff thin-plate theory.

In calculation, the plate dimensions are 100 × 100 mm and the thickness is 1.0 mm. The Young's modulus of material is E = 73.0 Gpa (Alclad 2024-T3), and the Poisson's ratio is ν = 0.33. The load caused by the loading pin is 80.0 N. These inputs are directly comparable to the experiments that will be discussed in the next section.

The boundary conditions of the model have been imposed as follows. Like a riveted joint, the top edge is free, whereas the fixed bottom edge is carrying loads. Both vertical edges of the plate are specified as simple supports identical to the experimental boundary conditions. The upper half-arc of the perimeter of the hole is free only in the loading direction (in the y direction).

The finite element arrangement for the cracked model consists of 184 nine-noded Lagrangian Mindlin plate elements, as shown in Fig. 2. The mesh used for an uncracked model is identical to the mesh for the cracked model, apart from the crack.

On plotting the predicted stress field obtained from FEM, for a pin-loading plate in which the crack length is 5 mm and the diameter

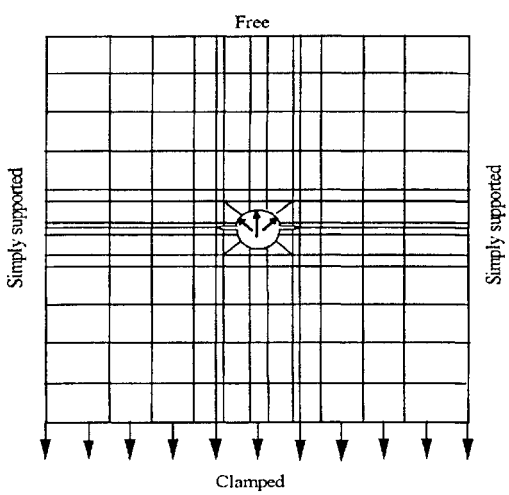

Fig. 2 Finite element model for cracked pin-loaded plate.

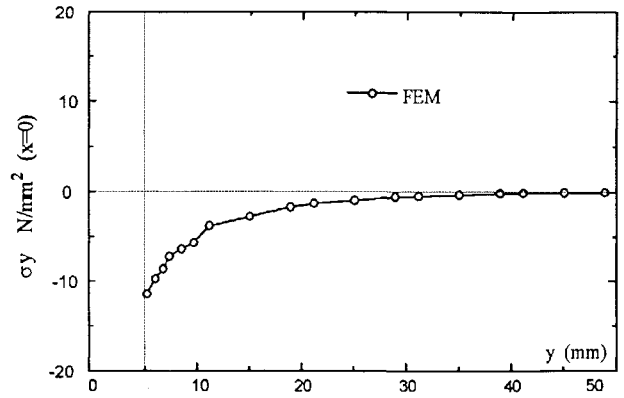

Fig. 3 Compressive stress (σ_y) distribution above the hole as a result of pin loading, x = 0.

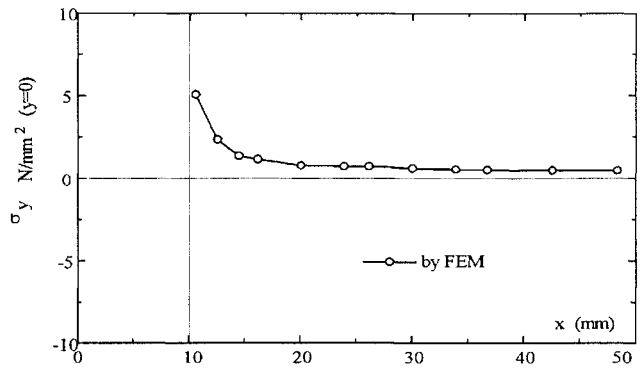

Fig. 4 Tensile stress (σ_y) distribution along the x axis, y = 0.

of the pin-loaded hole is 10.0 mm, it is found that most of the stress field is tensile. However, a region of high compressive stress is developed near the region of the top of the pin-loaded hole (that is immediately above the hole in Fig. 1), and a small region of high tensile stress is developed near the tip of the crack. Figures 3 and 4 show the expected results that the extent of the region of the compressive stresses near the region of the top of the pin-loaded hole is much greater than the extent of the tensile region near the crack.

Theoretically, the pressure load at the top of the pin $(0, r)$ should be $(2P)/(\pi r)$ by using cosine pressure distribution. However, when using FEM, two main approximations must be considered. First, the stresses are obtained by integrating the constitutive relationship at the element Gauss points. Nodal stresses, particularly stresses at the boundary, are then obtained by extrapolation from the Gauss points. Second, element nodal loads produced by external forces are obtained by numerical integration based on equilibrium or equivalent principle.

In Fig. 5, the predicted compressive stress distribution is plotted along the centerline above the pin-loaded hole for various crack lengths. It shows that the extent and magnitude of the compressive stresses near the region of the top of the pin-loaded hole decrease as the crack length is reduced. Note that, when the crack length is reduced to less than 1.0 mm, the extent and magnitude of the compressive stress region near the region of the top of the pin-loaded hole decrease rapidly. That is, the degree of the interference between contact stress and crack stress increases for cracks of less than 1.0 mm. This effect determines the interaction between buckling and fracture. It was found that σ_x as second main contributor is similar to σ_y, and it also affects the local buckling. Its effect is considered in local buckling analysis in the next section.

Local Buckling Calculation

The local buckling eigenvalues and eigenvectors were calculated using the subspace iteration method with the Rayleigh minimum principle expressed by Bathe and Wilson.[9]

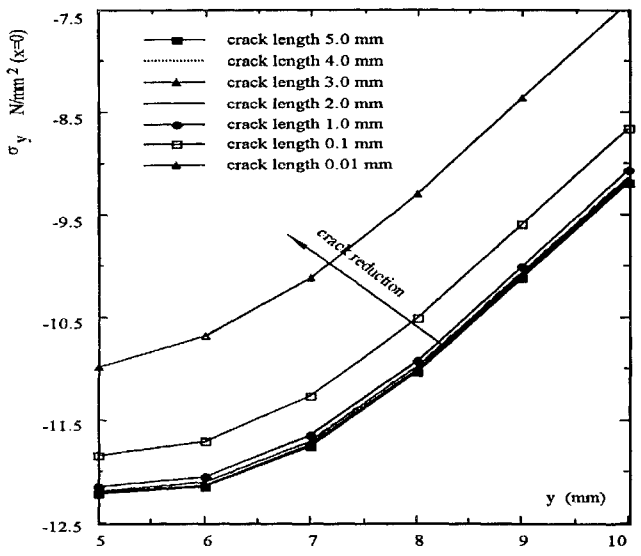

Fig. 5 Effect of crack length on compressive stress fields above the hole at a fixed load.

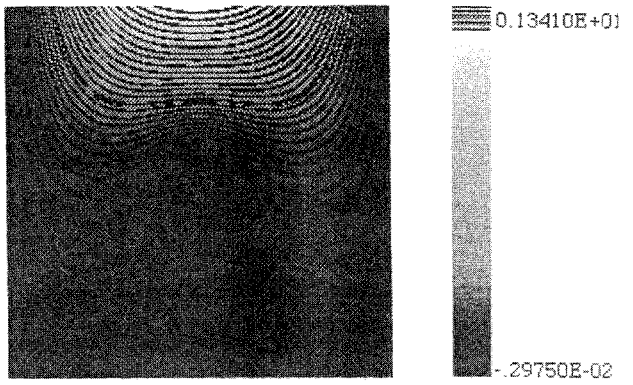

Fig. 6 Displacement contours (mm) for buckling mode 1 by FEM.

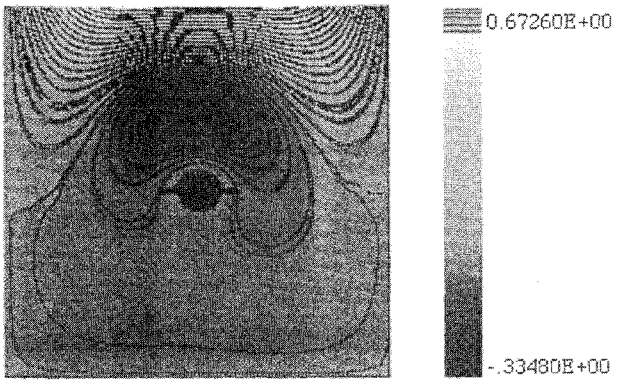

Fig. 7 Displacement contours (mm) for buckling mode 2 by FEM.

When the crack length a is 5 mm and the diameter of the pin-loaded hole is 10.0 mm, the predicted critical buckling loads are 78.2 N for buckling mode 1 and 140.4 N for buckling mode 2, as shown in Figs. 6 and 7, respectively.

The higher-order buckling loads and mode shapes can be calculated by the finite element program; however, the modes were of complex shapes, which were not observed in the experiments and have not been reported here.

Experimental Analysis

To measure the three-dimensional surface displacements that occur in local buckling, holospeckle interferometry has been used.[10–12] In the experimental arrangement, the laser light incident on the plate takes the place of the reference beam in conventional holography, and the light transmitted through the plate is reflected from the object and becomes the object beam. Interferometric fringes that result from out-of-plane displacement can be obtained by means of the double-exposure holographic technique.

To obtain reliable data for a buckling experiment, the following precautions were taken.

1) The plate support fixture was designed to keep the effect of geometrical imperfection as small as possible. The two parallel adjustable V-shaped slotted bars are used to simply support the vertical edges of the plate. The top pin load set applies the tensile load on the perimeter of the hole, and the bottom grip is the fixed support of the plate (the plate is free on its top edge, and no load is applied on the top edge).

2) All of the specimens in this study were machined such that their loading directions were parallel to the rolling direction of the sheet, avoiding anisotropy effects.

3) The screw driven crosshead of the loading machine provided precise displacement control. A crosshead speed of 5 mm/min was selected in this study. Flexible joints were used to ensure tensile load alignment.

The specimens tested in this investigation were all 1.0-mm-thick, aluminum alloy (Alclad 2024-T3) plates with a center hole. The diameter of the hole was 10.0 mm. The test section dimension of the specimen was 100 mm long $\times$100 mm wide. These parameters are directly comparable to the computational results that were explained in the foregoing section. The material of the pin used in the experiment is normal mild steel.

The buckling measurements involved two different procedures. The first is recording the holographic interferogram, whereas the second is the image analysis of the result. The holographic plate was attached to the test piece in two places. Using a tripod-mounted laser for illumination, the holographic plate was exposed twice, once at a minimal reference load and once at the given applied load. The minimal reference load was used to support the plate in the loading centerline to reduce the geometrical imperfection. The holographic plate was then developed. The resulting holographic interferogram then recorded out-of-plane displacements as fringes, visible in reflected white light, representing contours of the displacement. The holographic interferogram also recorded the two components of in-plane deformation that could be visualized in the diffraction of transmitted light.

The first test was designed to compare the differences of the displacements between buckled and unbuckled pin-loaded plates with no cracks. In Fig. 8, the 3.70-kN applied load does not cause local buckling; the hologram shows the measured out-of-plane displacements that occur between the reference load of 0.15 kN and the

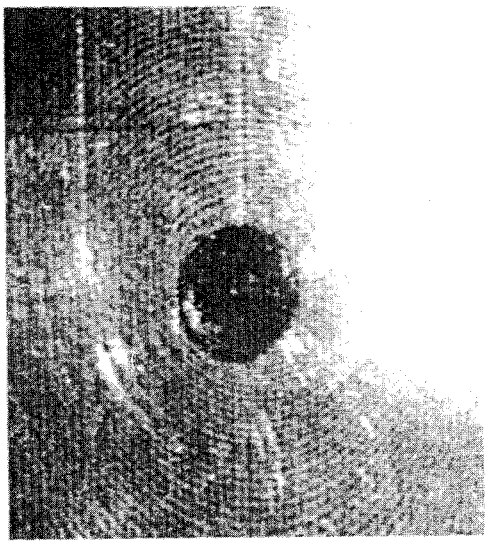

Fig. 8 Out-of-plane displacement pattern of the unbuckled pin-loaded plate.

Fig. 9 Out-of-plane displacement pattern of the buckled pin-loaded plate.

major applied load of 3.70 kN. The two in-plane displacement patterns indicate regions of high displacements gradient around the hole with evenly spaced displacement contours above the hole. Contrast these displacements with those shown in Fig. 9; the reference load is 0.03 kN and the applied load is now 4.24 kN. A local buckle is clearly visible above the hole in Fig. 9. Also, the in-plane displacements now indicate a concentration of displacement contours in the region of local buckling with a corresponding increase in the spacing of the displacement contours immediately adjacent to the hole. In the experiment, it is found that after local buckling, as the load increases further, the buckling region becomes very steep; viz., the out-of-plane displacement derivative in the local buckling region increases.

The local buckling mode observed in Fig. 9 is similar to buckling mode 2 as predicted by the finite element program and shown in Fig. 7. Buckling mode 1 was not observed in the experiments. The predicted buckling mode 1 shape, Fig. 6, shows a broad region of out-of-plane deformation above the hole and extending out to the edges of the sheet. The authors suspect that this pattern was too widespread to be readily detected by the holography method employed. Alternatively, it may be that buckling mode 1 is suppressed by slight imperfections in the flatness of the thin aluminum sheet employed in the experiments. Because of these considerations, it is assumed that the observed buckling shapes correspond to buckling mode 2.

Interaction of Fracture and Local Buckling

As discussed in the preceding sections, local buckling predictions and measurements for cracked and pin-loaded plates were obtained by utilizing finite element prediction and by using the holospeckle interferometry technique, respectively. In this section, the effects of crack length, boundary conditions, and diameter of the pin-loaded hole on local buckling loads and modes will be analyzed and discussed.

The first case studied is the effect of crack length by the aid of the FEM. The values of a/L, the ratio of crack length of plate width, are taken as 0.00 ($a = 0$), 0.01, 0.02, 0.03, 0.04, and 0.05. Results are presented in Table 1. When the value of a/L increases, the value of the critical buckling loads decreases. This is because the smaller the crack length is, the smaller is the prebuckling compressive stress near the top of the pin-loaded hole. This is shown in Fig. 5 obtained by the FEM.

Comparing with holospeckle interferometry technique, the effect of crack length on the critical buckling load is shown in Table 2. The tolerances indicate the accuracy of the determination of local buckling load, approximately ± 15 N as obtained by repeated experiments (the lower limit of the tolerances is the highest applied load

Table 1 Effect of a/L on the critical buckling loads (N)

a/L	Mode 1	Mode 2
0.00	112.328	199.442
0.01	99.091	178.677
0.02	93.790	168.190
0.03	88.487	163.218
0.04	83.075	154.198
0.05	78.229	140.361

Table 2 Critical buckling loads of mode 2 (N) obtained by FEM and by holospeckle interferometry

a/L	0.01	0.02	0.03	0.04	0.05
FEM	179	168	163	154	140
Test	350 ± 15	300 ± 15	265 ± 15	230 ± 15	200 ± 15

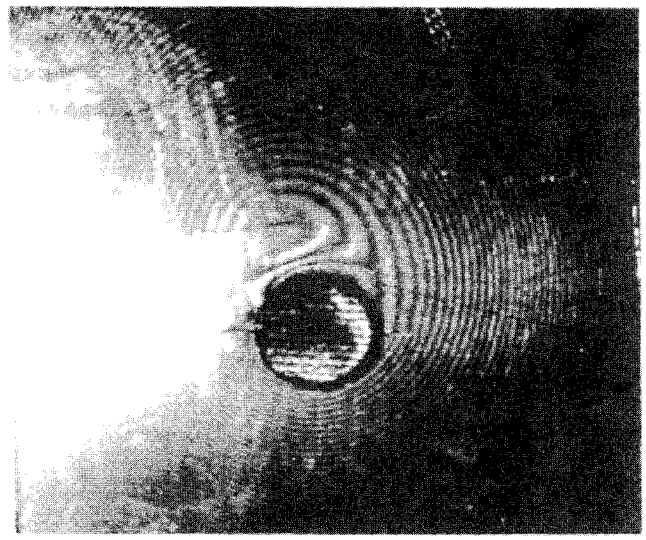

Fig. 10 Local buckling mode 2 of cracked and pin-loaded plate (a = 3.0 mm).

under which the plate is unbuckled; the upper limit of tolerances is the lowest applied load under which the plate buckles locally). One of their corresponding buckling modes obtained by holospeckle interferometry is shown in Fig. 10. The finite element predictions, based on buckling mode 2, are well below experimental results but follow a similar trend. It is thought that this inaccuracy is probably a result of difficulty in accurately representing, in the model, the boundary stress distribution and restraint conditions at the pin-loaded hole. Despite these shortcomings in the model, the effects of changing various modeling parameters are discussed next.

As crack length increases, the value of the critical buckling loads decreases. The longer the crack length is, the closer are the critical buckling loads obtained by holospeckle interferometry to the critical buckling loads obtained by the FEM. As discussed before, for the FEM approach, when crack length was reduced to less than 1.0 mm, the extent and magnitude of the region of compressive stress near the region of the top of the pin-loaded hole decrease drastically. That is, the degree of sensitivity of the buckling load to the crack length increases. The buckling load predicted by the FEM model was only slightly increased when the crack length was reduced to less than 1.0 mm. This is thought to be because the parabolic isoparametric Mindlin plate elements were not accurate enough to simulate the compressive stress region near the loading point. This sensitivity was confirmed in experiments but is not predicted by the finite element model.

The manner in which boundary conditions affect the critical buckling loads was also explored using the FEM. In the upper half-arc of the pin-loaded hole, different boundary conditions gave different critical loads. For instance, the second-order critical buckling loads for free in the z direction and fixed in the z direction are listed in

Table 3 Boundary effect on the critical buckling loads of mode 2 (N)

a/L	0.00	0.01	0.02	0.03	0.04	0.05
Free z	194.4	175.3	164.5	154.6	145.4	131.8
Fix z	199.4	178.7	168.2	163.2	154.2	140.4

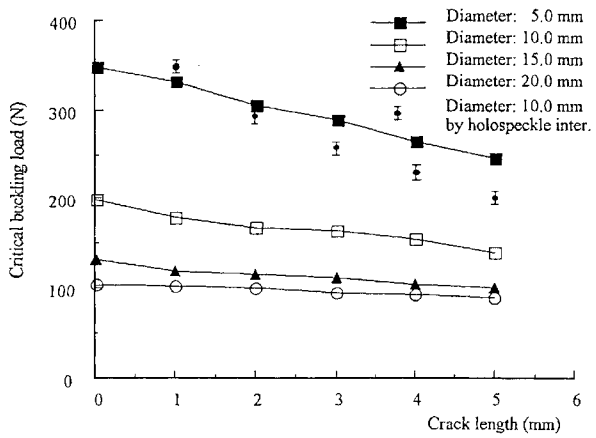

Fig. 11 Effect of diameter on critical buckling loads of mode 2.

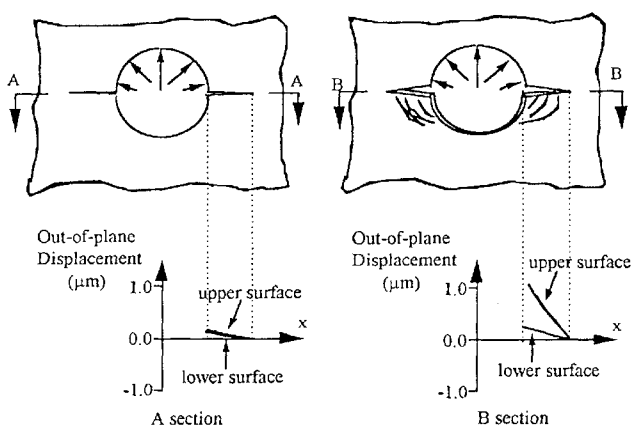

Fig. 12 Fracture mode change before and after local buckling.

Table 3 when the diameter of the hole is 10.0 mm. The first-order critical buckling loads for fixed in the z direction are larger than those for free in the z direction. However, this effect is relatively small. The effect was also small of higher-order buckling modes.

The effect of the pin-loaded hole diameter on the critical buckling loads is presented in Fig. 11. It is noticeable that the critical buckling load decreases as the diameter increases at the same crack length. Figure 11 also shows that the critical buckling loads for a pin-loaded hole of larger diameter is less sensitive to crack length than those for a smaller hole. As might be expected, the degree of the interference between contact stress and a crack of given length decreases when the hole is large. Conversely, for the case of a tiny crack and a small hole diameter, the degree of interaction is high and the difficulty of simulation with the finite element model increases.

With measurements of the local buckling modes obtained by holospeckle interferometry, the out-of-plane displacements immediately above the cracks are different from the displacements below the cracks after local buckling (see Fig. 10). That is, there is a discontinuity of the fringes across the cracks. This shows the existence of shearing at the cracks after local buckling. Comparing with the unbuckled mode (see Fig. 8), the local buckling makes the fracture mode change from purely opening mode 1 into a combined mode, opening mode 1 and tearing mode 3, as depicted in Fig. 12.

Conclusions

It may be concluded from the preceding numerical and experimental analyses that holospeckle interferometry and Mindlin element method are powerful tools for investigating fracture buckling of cracked and pin-loaded plates. In the stress analysis of cracked and pin-loaded plates, it has been shown that a high compressive stress concentration is developed near the region at the top of pin-loaded hole and a high tensile stress concentration near the crack tip. It has also been shown that the extent and the magnitude of the region of the compressive stresses at the region near the top of the pin-loaded hole decrease as the crack length is reduced. An important result was that, when the crack length was reduced to less than 1.0 mm, the extent and magnitude of the region of compressive stress at the top of the pin-loaded hole decrease rapidly. That is, the contact stress field was highly sensitive to crack length for small cracks.

Local buckling loads and modes were predicted and measured using holospeckle interferometry and the Mindlin plate FEM. A parametric study has shown that when crack length increases, the value of the critical buckling loads decreases, and the critical buckling loads for the pin-loaded hole of smaller diameter are more sensitive to the crack lengths than those for larger holes. This shows that there is a strong interaction between buckling and fracture under the circumstances investigated.

Using holospeckle interferometry, the fringe images have shown a change in the fracture mode after local buckling. Before local buckling, the fracture mode may be considered as opening mode 1; after local buckling, the fracture mode changes into a combined mode, opening mode 1 plus tearing mode 3. The fracture mode change may be an important factor in multisite damage failure in an aircraft fuselage.

References

[1]Leonelli, F. J., "Structural Airworthiness of New and Aging Aircraft," *5th International Conference on Structural Airworthiness of New and Aging Aircraft* (Hamburg, Germany), Deutsche Gesellschaft für Luft- und Rahmfahrt-Lilienthal-Oberth e.V., Bonn, Germany, 1993, pp. 33–36.

[2]Frostig, Y., Siton, G., Segal, A., Sheinman, I., and Weller, T., "Post-buckling Behaviour of Laminated Composite Stiffeners and Stiffened Panels Under Cyclic Loading," *Journal of Aircraft*, Vol. 28, No. 7, 1991, pp. 471–480.

[3]Rader, W., and McGregor, H., "Engineering Practices in the Solution of Acoustical Fatigue Problems for the Titans," *Acoustical Fatigue in Aerospace Structures*, edited by W. J. Trapp and D. Forney, Syracuse Univ. Press, Syracuse, NY, 1965, p. 707.

[4]Cherepanov, G. P., "On the Buckling Under Tension of a Membrane Containing Holes," *Journal of Applied Mathematics and Mechanics*, Vol. 27, 1963, pp. 405–420.

[5]Markstrom, K., and Storakers, B., "Buckling of Cracked Members Under Tension," *International Journal of Solids and Structures*, Vol. 16, No. 3, 1980, pp. 217–229.

[6]Sih, G. C., and Lee, Y. D., "Tensile and Compressive Buckling of Plates Weakened by Cracks," *Theoretical and Applied Fracture Mechanics*, Vol. 6, No. 2, 1986, pp. 129–138.

[7]Shaw, D., and Huang, Y. H., "Buckling Behaviour of a Central Cracked Thin Plate Under Tension," *Engineering Fracture Mechanics*, Vol. 35, No. 6, 1990, pp. 1019–1027.

[8]Zhuang, W. Z. L., Baird, J. P., and Williamson, H. M., "Finite Element Analysis of Local Buckling of a Cracked and Pin-Loaded Plate," *Computational Mechanics—From Concepts to Computations*, edited by S. Valliappan, V. A. Pulmano, and F. Tin-Loi, Vol. 1, Balkema, Rotterdam, The Netherlands, 1993, pp. 293–297.

[9]Bathe, K., and Wilson, E. L., *Numerical Methods in Finite Element Analysis*, Prentice-Hall, Englewood Cliffs, NJ, 1976.

[10]Zhuang, W. Z. L., Baird, J. P., Williamson, H. M., and Clark, R. K., "Three-Dimensional Displacement Measurement by a Holospeckle Interferometry Method," *Applied Optics*, Vol. 32, No. 25, 1993, pp. 4728–4737.

[11]Zhuang, W. Z. L., Baird, J. P., and Williamson, H. M., "A Optical Method for Local Buckling Measurement," *Proceedings of 1993 SEM "50th Anniversary" Spring Conference on Experimental Mechanics*, Society for Experimental Mechanics, Inc., Bethel, CT, 1993, pp. 451–459.

[12]Zhuang, W. Z. L., Baird, J. P., and Williamson, H. M., "Local Buckling Behaviour of a Cracked Rivet Joint," *Proceedings of 12th US National Congress of Applied Mechanics*, American Society of Mechanical Engineers, New York, 1994.